



Published in final edited form as:

J Am Chem Soc. 2017 March 22; 139(11): 3938–3941. doi:10.1021/jacs.6b13091.

Fast Hydrogen Atom Abstraction by a Hydroxo Iron(III) Porphyrzine

Hongxin Gao and John T. Groves*

Department of Chemistry, Princeton University, Princeton, New Jersey 08544, United States

Abstract

A reactive hydroxoferric porphyrzine complex, [(PyPz)Fe^{III}(OH)(OH₂)]⁴⁺ (**1**, PyPz = tetramethyl-2,3-pyridino porphyrzine), has been prepared via one-electron oxidation of the corresponding ferrous species [(PyPz)Fe^{II}(OH₂)₂]⁴⁺ (**2**). Electrochemical analysis revealed a pH-dependent and remarkably high Fe^{III}-OH/Fe^{II}-OH₂ reduction potential of 680 mV vs Ag/AgCl at pH 5.2. Nernstian behavior from pH 2 to pH 8 indicates a one-proton, one-electron interconversion throughout that range. The O–H bond dissociation energy of the Fe^{II}-OH₂ complex was estimated to be 84 kcal mol⁻¹. Accordingly, **1** reacts rapidly with a panel of substrates via C–H hydrogen atom transfer (HAT), reducing **1** to [(PyPz)Fe^{II}(OH₂)₂]⁴⁺ (**2**). The second-order rate constant for the reaction of [(PyPz)Fe^{III}(OH)(OH₂)]⁴⁺ with xanthene was 2.22 × 10³ M⁻¹ s⁻¹, 5–6 orders of magnitude faster than other reported Fe^{III}-OH complexes and faster than many ferryl complexes.

Nature has evolved a variety of remarkably efficient metalloenzymes for the selective oxygenation of even the most unreactive C–H bonds.¹ Copper-containing particulate methane monooxygenases (pMMO), and the nonheme diiron enzymes sMMO and AlkB allow microorganisms to grow on natural gas and petroleum as their sole sources of carbon.² Cytochrome P450s are thiolate-ligated heme proteins that use an oxoiron(IV)-porphyrin π -radical cation (compound I) as the active oxidant to functionalize substrates.³ Nonheme iron proteins such as TauD and SyrB2 break strong C–H bonds using a ferryl species, Fe^{IV}=O.⁴ By distinct contrast, lipoxygenases, which are widely distributed in plants, animals and fungi, employ hydroxoiron(III) or manganese(III) as reactive intermediates to activate allylic C–H bonds.⁵ These enzymes catalyze the regio- and stereospecific dioxygenation of polyunsaturated fatty acids to afford alkyl hydroperoxides. The use of enz-Fe^{III}-OH as a hydrogen atom transfer (HAT) agent to cleave the substrate C–H bond produces [enz-Fe^{II}-OH₂·R]. This strategy avoids the formation of high-valent intermediates and facilitates oxygen capture by the incipient substrate radical, ·R.

*Corresponding Author: jtgroves@princeton.edu.

Supporting Information

The Supporting Information is available free of charge on the ACS Publications website at DOI: 10.1021/jacs.6b13091. UV-vis and NMR spectra spectra, stopped-flow transients, kinetic traces and electrochemical data (PDF)

ORCID

John T. Groves: 0000-0002-9944-5899

Notes

The authors declare no competing financial interest.

Heme and nonheme oxoiron(IV) models have been extensively studied as hydrogen abstractors.^{4d,6} However, much less is known about the range of reactivity of hydroxometal(III) species, especially hydroxoiron(III). Notable early examples are hydroxoFe^{III}(PY5) complexes described by Stack et al.,⁷ and strongly hydrogen bonded terminal hydroxoiron(III) and manganese(III) species reported by Borovik et al.⁸ Mayer et al. have examined mechanisms of proton-coupled electron transfer with a hydroxoiron(III) porphyrin complex⁹ and recently, Tolman et al. have shown that a copper(III) hydroxide complex was highly reactive in C–H oxygenation reactions.¹⁰ An Fe(III) hydroxide complex described by Kovacs et al.¹¹ is an unusually weak oxidant and Jackson et al. have described phenol oxidations by mononuclear Mn^{III}–OH complexes.¹² Yet, with the exception of the high-valent Cu(III)–OH complex, the reaction rates of hydrogen atom abstraction by these metal(III) hydroxide species are very slow compared with lipoygenases.^{5f,13}

We describe here the generation and reactions of a cationic hydroxoferric complex, [(PyPz)Fe^{III}(OH)(OH₂)]⁴⁺ (**1**, PyPz = tetramethyl-2,3-pyridino porphyrazine, Scheme 1) that is capable of fast hydrogen atom abstractions from substrates with moderate C–H bond energies (<85 kcal mol⁻¹). The ferric complex is reduced to [(PyPz)Fe^{II}(OH₂)₂]⁴⁺ (**2**) for which an O–H BDE of 84 kcal mol⁻¹ was estimated from the Fe^{III}/Fe^{II} reduction potential. Second-order rate constants for C–H hydrogen atom abstraction by **1** are orders of magnitude faster than other reported ferric complexes.

The ferrous complex **2** was prepared by heating pyridine-2,3-dicarboxylic acid with urea and ferrous chloride with ammonium heptamolybdate as a catalyst, followed by *N*-methylation with methyl *p*-toluenesulfonate as previously described.¹⁴ Complex **2** showed an appropriate molecular ion in the ESI MS (Figure S1) and sharp peaks in the ¹H NMR with similar chemical shifts to those of Zn^{II}PyPz (Figure S2).¹⁵ The EPR spectrum of **2** showed no signals (Figure S3). On the basis of these results, air-stable complex **2** is formulated as a diamagnetic, low-spin ferrous complex [(PyPz)Fe^{II}(OH₂)₂]⁴⁺.¹⁶ Titration of **2**, as monitored by UV–vis spectroscopy (Figure S4), showed two successive deprotonations of axial water with p*K*_{a1} = 8.0 and p*K*_{a2} = 10.1, indicative of diaqua, aqua-hydroxo and dihydroxo coordination of iron(II).^{6i,17}

Cyclic voltammetry of **2** afforded a pH-dependent redox potential with a slope of –69 mV/pH in the Pourbaix diagram between pH 2.2 and 7.7 (Figure S5), close to the expected –59 mV/pH for ideal Nernstian behavior.^{11,18} Further, the *E*_{pa} – *E*_{pc} difference at pH 2.2 decreased as the scan rate decreased, with a *E* of 68 mV at 2 mV/s (Figure S6 and Table S1). This behavior is indicative of the transfer one proton per electron and that the ferric complex **1** has one hydroxo and one aqua axial ligand over this entire pH range. The redox potential of Fe(III/II)PyPz is 680 mV vs Ag/AgCl at pH 5.2, unusually high for a Fe^{III}/Fe^{II} couple, explaining the stability of **2** in air.

The ferrous complex **2** could be oxidized to complex **1** either by bulk electrolysis at 1 V (vs Ag/AgCl) or by adding one equivalent of *t*-butyl hydroperoxide, as monitored by UV–vis spectroscopy at pH 2.2 (Figure S7). The EPR spectrum of complex **1** (*g* = 2.49, 2.21, 1.89) indicates that **1** can be formulated as a low-spin ferric complex [(PyPz)Fe^{III}(OH)(OH₂)]⁴⁺ (Figure S3).¹⁹

The strength of the O–H bond in transition metal complexes is of considerable importance in determining the driving force for hydrogen atom abstraction.²⁰ Because the redox potential of **1/2** is pH-dependent, the $D(\text{O–H})$ of **2** could be calculated using the modified form of the Bordwell eq (eq 1):

$$D(\text{O–H}) = 23.06E_{1/2} + 1.37\text{pH} + C \text{ kcal/mol} \quad (1)$$

where $E_{1/2}$ is the oxidation potential of **2** (referenced to NHE, Ag/AgCl + 220 mV) at a given pH and C is the solvent-dependent energy of formation and solvation of H in H₂O, which equals to 55.8 kcal mol⁻¹.^{20b,21} With the exceptionally high Fe^{III}/Fe^{II} redox potential of the **1/2** couple, $D(\text{O–H})$ in **2** is calculated to be 84 ± 2 kcal mol⁻¹, suggesting that **1** should be capable of oxidizing C–H substrates with moderate C–H bond strengths.

Indeed, the decay of (PyPz)Fe^{III}–OH to (PyPz)Fe^{II}–OH₂ was greatly accelerated by added substrates. The kinetics monitored at 453 nm by stopped-flow spectrophotometry for a panel of C–H substrates were very well fit by single exponentials over a range of substrate concentrations as expected for a pseudo-first order reduction of **1** to **2** (Figure 1). The second-order rate constant for xanthene oxidation was remarkably fast; $k = 2216 \pm 28 \text{ M}^{-1} \text{ s}^{-1}$. For xanthene-*d*₂, the value was $109.7 \pm 0.6 \text{ M}^{-1} \text{ s}^{-1}$, indicative of a very large substrate kinetic isotope effect (KIE) of 20.2 ± 0.3 . Clearly, cleavage of the C–H bond is the rate-determining step. Conversely, the solvent isotope effect was negligible (Figure 1B).^{6h}

A correlation of the reduction of **1** by a panel of five substrates is plotted versus the C–H BDE in Figure 2. A linear Brønsted–Evans–Polanyi (BEP) relationship was found with a slope of -0.35 , indicating a homolytic hydrogen atom transfer with an early transition state.^{6e,20c,22} Similar results were obtained in phosphate buffer/acetonitrile solution at both acidic (Figure S8–12) and near-neutral pH (Figure S13–15), with very little pH sensitivity up to pH 7.2 (Figure S16).

The reaction of (PyPz)Fe^{III}–OH with xanthene was examined in greater detail. A KIE of 20.2 at 293 K is significantly greater than the semiclassical limit of 7. Analyzing Arrhenius plots for xanthene and xanthene-*d*₂ oxidation by **1** gave $E_a(\text{D}) - E_a(\text{H}) = 2.5 \pm 0.4 \text{ kcal mol}^{-1}$ and $A(\text{H})/A(\text{D}) = 0.28 \pm 0.14$ (Figure S17). These results meet all three Kreevoy criteria for hydrogen tunneling: a KIE significantly larger than 6.4 at 20 °C; an activation energy difference greater than 1.2 kcal mol⁻¹; and a ratio of pre-exponential factors less than 0.7.²³ This large KIE of 20.2 is much greater than those reported for other synthetic ferric hydroxide complexes, and closer to the colossal KIE of ~80 found for lipoxygenases.^{7d,24}

An Eyring analysis of the temperature dependence of the rate constants gave remarkably small enthalpies of activation; $H^\ddagger = 6.1 \pm 0.3 \text{ kcal mol}^{-1}$ and $S^\ddagger = -23.7 \pm 1.1 \text{ cal mol}^{-1} \text{ K}^{-1}$ for xanthene and $H^\ddagger = 6.8 \pm 0.3 \text{ kcal mol}^{-1}$, $S^\ddagger = -27.2 \pm 0.8 \text{ cal mol}^{-1} \text{ K}^{-1}$ for 9,10-dihydroanthracene (DHA) (Figure S18). Accordingly, C–H scission occurs under entropy control with $T S^\ddagger > H^\ddagger$. Notably, the enthalpy barrier for lipoxygenase is only 2 kcal mol⁻¹, resulting in the very fast rate of the enzyme.²⁵

The unusually high reactivity of this hydroxoferric porphyrzine complex (**1**) prompts a comparison of C–H bond cleavage rates with other hydroxometal(III) and oxoiron(IV) complexes, as well as organic radicals. Figure 3 shows such a comparison for DHA oxidation at 25 °C by various complexes versus the $D(O-H)$ values associated with the oxidants.^{6a,c,h,k,7,10a,b,18,26} For calibration, the dashed line passes through rates with known $D(O-H)$ for permanganate, the *t*-butylperoxyl radical and the *t*-butoxyl radical (not shown).^{26a-d,27} Although the O–H BDE associated with **1/2** is only a few kcal mol⁻¹ stronger than other synthetic hydroxo-manganese(III) and iron(III) complexes, the rate of **1/2** is 5 to 6 orders of magnitude faster. Moreover, this rate is 50–100-fold faster than typical ferryl complexes and comparable to that of the PINO radical, *t*-butylperoxy radical and a hydroxocopper(III) complex.^{10b,26e} Much faster rates of DHA oxidation have been reported for oxoiron(IV) porphyrin cation radicals^{6e,h} and for a high-spin ferryl species.^{26j}

What factors contribute to the high HAT reactivity of (PyPz)Fe^{III}-OH (**1**)? Certainly, part of the acceleration derives from the unusually high Fe^{III}/Fe^{II} redox potential. We note that the Fe^{IV}-OH (compound II) of the heme-thiolate peroxygenase APO is also highly reactive toward C–H bond scission despite its modest (0.84 V vs NHE) reduction potential.⁶ⁱ On the other hand, oxoFe^{IV}-4-TMPyP, a cationic porphyrin similar to **1** with four methylpyridinium positive charges, oxidizes xanthene at a rate more than 1 order of magnitude slower than the hydroxoferric species **1**.²⁸ A small reorganization energy for reduction of **1** to **2** might derive from the low-spin configuration of both species and the rather rigid porphyrzine ring system. The significant hydrogen tunneling contributes a factor of ~3. These factors suggest that some iron hydroxides may have intrinsically lower reorganization energies than corresponding ferryl species, reflecting less drastic bond-order changes. The possibility of a disproportionation of the ferric complex **1** to generate a reactive ferryl species is highly unlikely given the near-perfect fit of the kinetic data to a single exponential ($R^2 = 0.9997$) over six half-lives of reaction and the tight isosbestic point at 407 nm (Figure 1A). Disproportionation processes should be second-order in Fe^{III}-OH (Figure S19).

In summary, we have found that the hydroxoferric porphyrzine complex, [(PyPz)Fe^{III}(OH)(OH₂)]⁴⁺ (**1**), is unusually reactive toward hydrogen abstraction from benzylic C–H substrates. The reactions occur through a hydrogen atom transfer mechanism, which is supported by the large KIE and a linear relationship between substrate C–H BDE and log *k*. A (PyPz)Fe^{II}-OH₂ O–H BDE of 84 kcal mol⁻¹ is estimated from the redox potential of (PyPz)Fe^{III}-OH/(PyPz)Fe^{II}-OH₂ and the pK_a of the axial aqua ligand of (PyPz)Fe^{II}. The shallow BEP slope (–0.35) indicates an early transition state for C–H scission and the low activation enthalpies ($H^\ddagger = 6.1\text{--}6.8$ kcal/mol) show that the reaction is entropy controlled ($T S^\ddagger > H^\ddagger$), suggesting a small reorganization energy for this process. These findings provide new insights into the reactivity of Fe^{III}-OH species and suggest that M–OH oxidants may have untapped potential in the context of C–H activation.

Supplementary Material

Refer to Web version on PubMed Central for supplementary material.

Acknowledgments

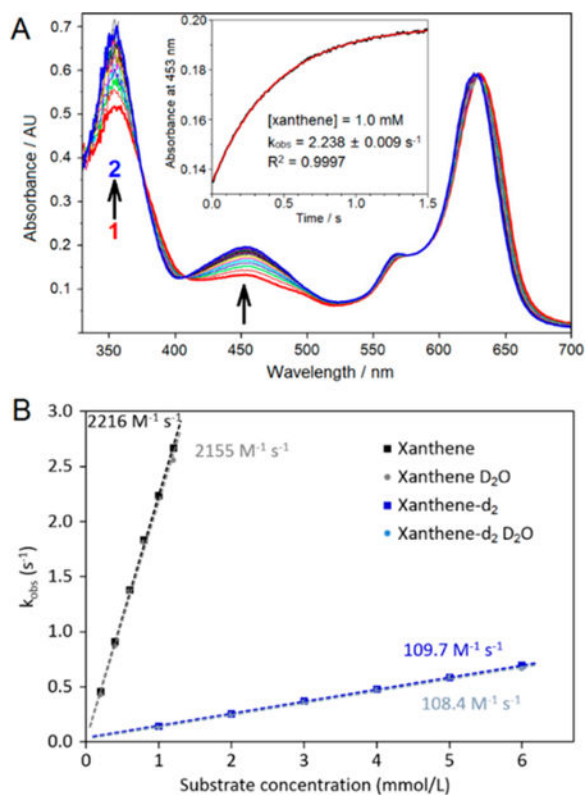
Support of this work was provided by the National Institutes of Health (2R37 GM036298).

References

- Huang X, Groves JT. *JBIC, J Biol Inorg Chem*. 2017; doi: 10.1007/s00775-016-1414-3
- (a) Lipscomb JD. *Annu Rev Microbiol*. 1994; 48:371. [PubMed: 7826011] (b) Citek C, Gary JB, Wasinger EC, Stack TD. *J Am Chem Soc*. 2015; 137:6991. [PubMed: 26020834] (c) Lieberman RL, Rosenzweig AC. *Nature*. 2005; 434:177. [PubMed: 15674245] (d) Tinberg CE, Lippard SJ. *Acc Chem Res*. 2011; 44:280. [PubMed: 21391602] (e) Cooper HLR, Mishra G, Huang X, Pender-Cudlip M, Austin RN, Shanklin J, Groves JT. *J Am Chem Soc*. 2012; 134:20365. [PubMed: 23157204]
- (a) Ortiz de Montellano PR. *Chem Rev*. 2010; 110:932. [PubMed: 19769330] (b) Shaik S, Cohen S, Wang Y, Chen H, Kumar D, Thiel W. *Chem Rev*. 2010; 110:949. [PubMed: 19813749] (c) Yosca TH, Rittle J, Krest CM, Onderko EL, Silakov A, Calixto JC, Behan RK, Green MT. *Science*. 2013; 342:825. [PubMed: 24233717] (d) Groves JT. *Proc Natl Acad Sci U S A*. 2003; 100:3569. [PubMed: 12655056] (e) Groves JT. *J Inorg Biochem*. 2006; 100:434. [PubMed: 16516297] (f) Krest CM, Silakov A, Rittle J, Yosca TH, Onderko EL, Calixto JC, Green MT. *Nat Chem*. 2015; 7:696. [PubMed: 26291940] (g) Rittle J, Green MT. *Science*. 2010; 330:933. [PubMed: 21071661] (h) Groves JT. *Nat Chem*. 2014; 6:89. [PubMed: 24451580]
- (a) Price JC, Barr EW, Tirupati B, Bollinger JM, Krebs C. *Biochemistry*. 2003; 42:7497. [PubMed: 12809506] (b) Blasiak LC, Vaillancourt FH, Walsh CT, Drennan CL. *Nature*. 2006; 440:368. [PubMed: 16541079] (c) Galoni Fujimori D, Barr EW, Matthews ML, Koch GM, Yonce JR, Walsh CT, Bollinger JM, Krebs C, Riggs-Gelasco PJ. *J Am Chem Soc*. 2007; 129:13408. [PubMed: 17939667] (d) Biswas AN, Puri M, Meier KK, Oloo WN, Rohde GT, Bominaar EL, Münck E, Que L. *J Am Chem Soc*. 2015; 137:2428. [PubMed: 25674662]
- (a) Collazo L, Klinman JP. *J Biol Chem*. 2016; 291:9052. [PubMed: 26867580] (b) Wennman A, Oliw EH, Karkehabadi S, Chen Y. *J Biol Chem*. 2016; 291:8130. [PubMed: 26783260] (c) Samuelsson B, Dahlen S, Lindgren J, Rouzer C, Serhan C. *Science*. 1987; 237:1171. [PubMed: 2820055] (d) Boyington J, Gaffney B, Amzel L. *Science*. 1993; 260:1482. [PubMed: 8502991] (e) Su C, Oliw EH. *J Biol Chem*. 1998; 273:13072. [PubMed: 9582345] (f) Knapp MJ, Klinman JP. *Biochemistry*. 2003; 42:11466. [PubMed: 14516198]
- (a) Kaizer J, Klinker EJ, Oh NY, Rohde JU, Song WJ, Stubna A, Kim J, Münck E, Nam W, Que L. *J Am Chem Soc*. 2004; 126:472. [PubMed: 14719937] (b) Jackson TA, Rohde JU, Seo MS, Sastri CV, DeHont R, Stubna A, Ohta T, Kitagawa T, Münck E, Nam W, Que L. *J Am Chem Soc*. 2008; 130:12394. [PubMed: 18712873] (c) Cho K, Leeladee P, McGown AJ, DeBeer S, Goldberg DP. *J Am Chem Soc*. 2012; 134:7392. [PubMed: 22489757] (d) Chen Z, Yin G. *Chem Soc Rev*. 2015; 44:1083. [PubMed: 25566588] (e) Bell SR, Groves JT. *J Am Chem Soc*. 2009; 131:9640. [PubMed: 19552441] (f) Wang X, Peter S, Kinne M, Hofrichter M, Groves JT. *J Am Chem Soc*. 2012; 134:12897. [PubMed: 22827262] (g) Wang X, Peter S, Ullrich R, Hofrichter M, Groves JT. *Angew Chem, Int Ed*. 2013; 52:9238. (h) Boaz NC, Bell SR, Groves JT. *J Am Chem Soc*. 2015; 137:2875. [PubMed: 25651467] (i) Wang X, Ullrich R, Hofrichter M, Groves JT. *Proc Natl Acad Sci USA*. 2015; 112:3686. [PubMed: 25759437] (j) Usharani D, Lacy DC, Borovik AS, Shaik S. *J Am Chem Soc*. 2013; 135:17090. [PubMed: 24124906] (k) Jeong YJ, Kang Y, Han AR, Lee YM, Kotani H, Fukuzumi S, Nam W. *Angew Chem, Int Ed*. 2008; 47:7321.
- (a) Jonas RT, Stack TDP. *J Am Chem Soc*. 1997; 119:8566. (b) Goldsmith CR, Jonas RT, Stack TDP. *J Am Chem Soc*. 2002; 124:83. [PubMed: 11772065] (c) Goldsmith CR, Cole AP, Stack TDP. *J Am Chem Soc*. 2005; 127:9904. [PubMed: 15998097] (d) Goldsmith CR, Stack TDP. *Inorg Chem*. 2006; 45:6048. [PubMed: 16842013]
- (a) Cook SA, Borovik AS. *Acc Chem Res*. 2015; 48:2407. [PubMed: 26181849] (b) Gupta R, Borovik AS. *J Am Chem Soc*. 2003; 125:13234. [PubMed: 14570499] (c) Gupta R, Taguchi T, Borovik AS, Hendrich MP. *Inorg Chem*. 2013; 52:12568. [PubMed: 24156406]
- Porter TR, Mayer JM. *Chem Sci*. 2014; 5:372. [PubMed: 24729854]

10. (a) Donoghue PJ, Tehranchi J, Cramer CJ, Sarangi R, Solomon EI, Tolman WB. *J Am Chem Soc.* 2011; 133:17602. [PubMed: 22004091] (b) Dhar D, Tolman WB. *J Am Chem Soc.* 2015; 137:1322. [PubMed: 25581555] (c) Dhar D, Yee GM, Spaeth AD, Boyce DW, Zhang H, Dereli B, Cramer CJ, Tolman WB. *J Am Chem Soc.* 2016; 138:356. [PubMed: 26693733]
11. Brines LM, Coggins MK, Poon PCY, Toledo S, Kaminsky W, Kirk ML, Kovacs JA. *J Am Chem Soc.* 2015; 137:2253. [PubMed: 25611075]
12. (a) Wijeratne GB, Corzine B, Day VW, Jackson TA. *Inorg Chem.* 2014; 53:7622. [PubMed: 25010596] (b) Wijeratne GB, Day VW, Jackson TA. *Dalton Trans.* 2015; 44:3295. [PubMed: 25597362] (c) Rice DB, Wijeratne GB, Burr AD, Parham JD, Day VW, Jackson TA. *Inorg Chem.* 2016; 55:8110. [PubMed: 27490691]
13. Knapp MJ, Seebeck FP, Klinman JP. *J Am Chem Soc.* 2001; 123:2931. [PubMed: 11457000]
14. Safari N, Jamaat PR, Shirvan SA, Shoghpour S, Ebadi A, Darvishi M, Shaabani A. *J Porphyryns Phthalocyanines.* 2005; 09:256.
15. Wohrle D, Gitzel J, Okura I, Aono S. *J Chem Soc, Perkin Trans 2.* 1985; 1171
16. (a) Appleby AJ, Fleisch J, Savy M. *J Catal.* 1976; 44:281.(b) Ercolani C, Gardini M, Murray KS, Pennesi G, Rossi G. *Inorg Chem.* 1986; 25:3972.(c) Tanaka AA, Fierro C, Scherson D, Yaeger EB. *J Phys Chem.* 1987; 91:3799.(d) Dieing R, Schmid G, Witke E, Feucht C, Dreßen M, Pohmer J, Hanack M. *Chem Ber.* 1995; 128:589.
17. (a) Ferrer-Sueta G, Vitturi D, Batini -Haberle I, Fridovich I, Goldstein S, Czapski G, Radi R. *J Biol Chem.* 2003; 278:27432. [PubMed: 12700236] (b) Lahaye D, Groves JT. *J Inorg Biochem.* 2007; 101:1786. [PubMed: 17825916]
18. Wang D, Zhang M, Bühlmann P, Que L. *J Am Chem Soc.* 2010; 132:7638. [PubMed: 20476758]
19. (a) Groves JT, Quinn R, McMurry TJ, Lang G, Boso B. *J Chem Soc, Chem Commun.* 1984:1455. (b) Kobayashi N, Shirai H, Hojo N. *J Chem Soc, Dalton Trans.* 1984:2107.(c) Ukita S, Fujii T, Hira D, Nishiyama T, Kawase T, Migita CT, Furukawa K. *FEMS Microbiol Lett.* 2010; 313:61. [PubMed: 20883501]
20. (a) Roth JP, Yoder JC, Won TJ, Mayer JM. *Science.* 2001; 294:2524. [PubMed: 11752572] (b) Warren JJ, Tronic TA, Mayer JM. *Chem Rev.* 2010; 110:6961. [PubMed: 20925411] (c) Mayer JM. *Acc Chem Res.* 2011; 44:36. [PubMed: 20977224]
21. Bordwell FG. *Acc Chem Res.* 1988; 21:456.
22. (a) Evans MG, Polanyi M. *Trans Faraday Soc.* 1938; 34:11.(b) Mayer JM. *Acc Chem Res.* 1998; 31:441.
23. (a) Kwart H. *Acc Chem Res.* 1982; 15:401.(b) Kim Y, Kreevoy MM. *J Am Chem Soc.* 1992; 114:7116.(c) Lewandowska-Andralojc A, Grills DC, Zhang J, Bullock RM, Miyazawa A, Kawanishi Y, Fujita E. *J Am Chem Soc.* 2014; 136:3572. [PubMed: 24498925]
24. (a) Cowley RE, Eckert NA, Vaddadi S, Figg TM, Cundari TR, Holland PL. *J Am Chem Soc.* 2011; 133:9796. [PubMed: 21563763] (b) Carr CAM, Klinman JP. *Biochemistry.* 2014; 53:2212. [PubMed: 24641705] (c) Hu S, Sharma SC, Scouras AD, Soudackov AV, Carr CAM, Hammes-Schiffer S, Alber T, Klinman JP. *J Am Chem Soc.* 2014; 136:8157. [PubMed: 24884374] (d) Layfield JP, Hammes-Schiffer S. *Chem Rev.* 2014; 114:3466. [PubMed: 24359189]
25. (a) Jonsson T, Glickman MH, Sun S, Klinman JP. *J Am Chem Soc.* 1996; 118:10319.(b) Knapp MJ, Rickert K, Klinman JP. *J Am Chem Soc.* 2002; 124:3865. [PubMed: 11942823]
26. (a) Arends IWCE, Mulder P, Clark KB, Wayner DDM. *J Phys Chem.* 1995; 99:8182.(b) Gardner KA, Kuehnert LL, Mayer JM. *Inorg Chem.* 1997; 36:2069. [PubMed: 11669825] (c) Wang K, Mayer JM. *J Am Chem Soc.* 1997; 119:1470.(d) Roth JP, Mayer JM. *Inorg Chem.* 1999; 38:2760. [PubMed: 11671018] (e) Koshino N, Saha B, Espenson JH. *J Org Chem.* 2003; 68:9364. [PubMed: 14629158] (f) Brandi P, Galli C, Gentili P. *J Org Chem.* 2005; 70:9521. [PubMed: 16268628] (g) Sastri CV, Lee J, Oh K, Lee YJ, Lee J, Jackson TA, Ray K, Hirao H, Shin W, Halfen JA, Kim J, Que L, Shaik S, Nam W. *Proc Natl Acad Sci U S A.* 2007; 104:19181. [PubMed: 18048327] (h) Fertinger C, Hessenauer-Ilicheva N, Franke A, van Eldik R. *Chem - Eur J.* 2009; 15:13435. [PubMed: 19876973] (i) England J, Martinho M, Farquhar ER, Frisch JR, Bominaar EL, Münck E, Que L. *Angew Chem, Int Ed.* 2009; 48:3622.(j) Puri M, Biswas AN, Fan R, Guo Y, Que L. *J Am Chem Soc.* 2016; 138:2484. [PubMed: 26875530]

27. We have used BDE values instead of BDFE to facilitate comparisons with other systems. Entropic effects due to electronic reorganization should be small because both 1 and 2 are low-spin. The aqueous BDFE for 2 would be ~2 kcal/mol larger, reflecting the difference between C_H and C_G in eq 1 (cf. references ^{10c}, ¹¹ and ^{20b}).
28. Bell, SR. PhD Thesis Princeton University; Princeton, NJ: 2010 Modeling Heme Monooxygenases with Water-Soluble Iron Porphyrins.

**Figure 1.**

(A) Single-mixing, stopped-flow UV-vis spectra obtained upon mixing 1.0 mM xanthene with $70 \mu\text{M}$ (PyPz)Fe^{III}-OH (**1**) in 50:50 (v/v) 6 mM HClO₄ water/acetonitrile solution (pH 2.2) at 20.0 °C over 1.5 s. Inset: changes in absorbance at 453 nm vs time (black line). Single exponential fitting (red line) resulted in a pseudo-first-order rate constant of $2.238 \pm 0.009 \text{ s}^{-1}$ ($R^2 = 0.9997$). (B) Observed pseudo-first-order rate constants plotted vs xanthene concentration: xanthene in H₂O: $2216 \pm 28 \text{ M}^{-1} \text{ s}^{-1}$ ($R^2 = 0.9992$) (black). Xanthene-*d*₂ in H₂O: $109.7 \pm 0.6 \text{ M}^{-1} \text{ s}^{-1}$ ($R^2 = 0.9998$), substrate KIE = 20.2 ± 0.3 (blue). Xanthene in D₂O: $2155 \pm 62 \text{ M}^{-1} \text{ s}^{-1}$ ($R^2 = 0.996$), solvent KIE = 1.03 ± 0.04 (gray). Xanthene-*d*₂ in D₂O: $108.4 \pm 2.8 \text{ M}^{-1} \text{ s}^{-1}$ ($R^2 = 0.997$), combined substrate-solvent KIE = 20.4 ± 0.6 (light blue).

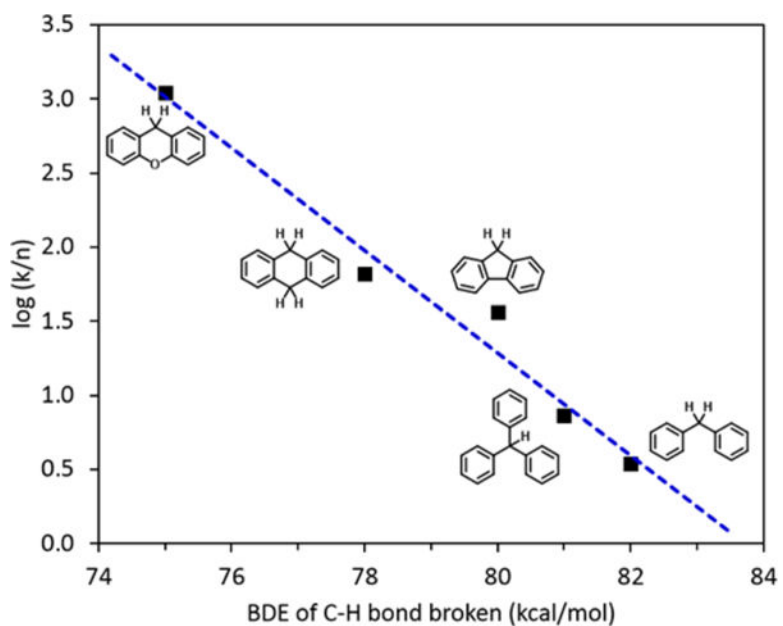


Figure 2. Plot of $\log(k/n)$ vs substrate BDE, where k is the second-order rate constant and n is the number of equivalent C–H bonds that are broken in the reaction. Conditions: $T = 20.0$ °C, 50:50 (v/v) 6 mM HClO_4 water/acetonitrile solution (pH 2.2). Slope = -0.35 ± 0.04 ($R^2 = 0.961$).

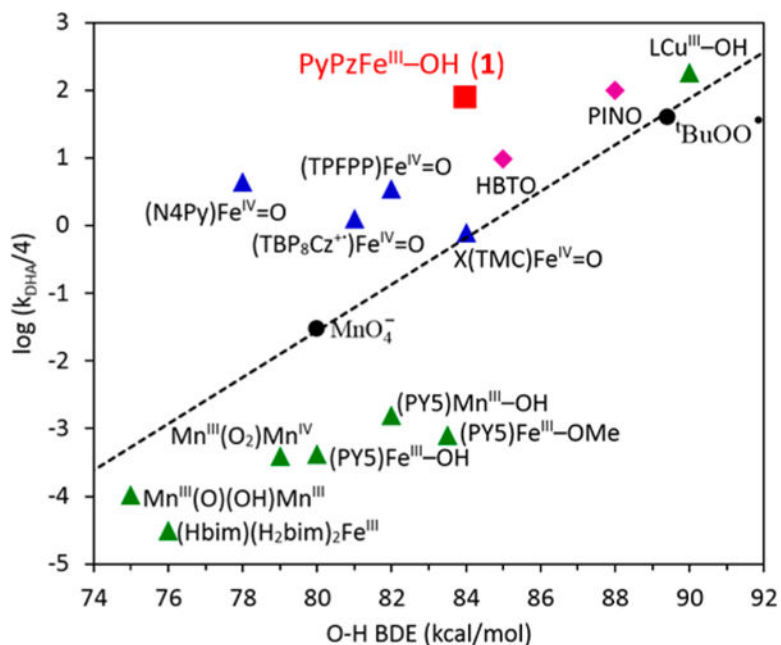
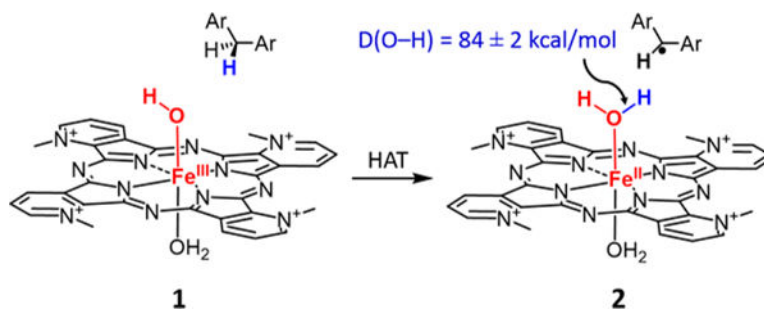


Figure 3.

Plot of $\log k$ for DHA oxidation and the O–H BDE formed by a variety of oxidants at 298 K. Rates were either measured directly or extrapolated to this temperature from experimentally determined activation parameters (Table S2). The black dashed line was drawn through the points of two oxygen radicals and permanganate as a reference. The red square is $(\text{PyPz})\text{Fe}^{\text{III}}\text{-OH}$ (**1**). Green triangles are reported metal(III) complexes. Blue triangles are reported $\text{Fe}^{\text{IV}}\text{=O}$ complexes. Magenta diamonds are organic oxy-radicals. An N–H bond is formed instead of O–H bond in $\text{Fe}^{\text{III}}(\text{Hbim})(\text{H}_2\text{bim})_2$. Data points of HBTO and PINO radicals are estimated from fluorene oxidation rates.

**Scheme 1.**

Conversion of [(PyPz)Fe^{III}(OH)(OH₂)]⁴⁺ (1) to [(PyPz)Fe^{II}(OH₂)₂]⁴⁺ (2) via HAT